Icarus xxx (2010) xxx–xxx

Contents lists available at ScienceDirect

Icarus

journal homepage: www.elsevier.com/locate/icarus

Molecular hydrogen in Titan's atmosphere: Implications of the measured tropospheric and thermospheric mole fractions

Darrell F. Strobel *

Department of Earth and Planetary Sciences, 3400 N. Charles Street, Johns Hopkins University, Baltimore, MD 21218, United States

ARTICLE INFO

Article history:
Received 11 January 2010
Revised 23 February 2010
Accepted 4 March 2010
Available online xxxx

Keywords:
Titan
Aeronomy
Atmospheres, Composition
Atmospheres, Structure

ABSTRACT

The third most abundant species in Titan's atmosphere is molecular hydrogen with a tropospheric/lower stratospheric mole fraction of 0.001 derived from Voyager and Cassini infrared measurements. The globally averaged thermospheric H_2 mole fraction profile from the Cassini Ion Neutral Mass Spectrometer (INMS) measurements implies a small positive gradient in the H_2 mixing ratio from the tropopause region to the lower thermosphere (~950–1000 km), which drives a downward H_2 flux into Titan's surface comparable to the H_2 escape flux out of the atmosphere ($\sim 2 \times 10^{10}$ cm^{-2} s^{-1} referenced to the surface) and requires larger photochemical production rates of H_2 than obtained by previous photochemical models. From detailed model calculations based on known photochemistry with eddy, molecular, and thermal diffusion, the tropospheric and thermospheric H_2 mole fractions are incompatible by a factor of ~2. The measurements imply that the downward H_2 surface flux is in substantial excess of the speculative threshold value for methanogenic life consumption of H_2 (McKay, C.P., Smith, H.D. [2005], Icarus 178, 274–276. doi:10.1016/j.icarus.2005.05.018), but without the extreme reduction in the surface H_2 mixing ratio.

© 2010 Elsevier Inc. All rights reserved.

1. Introduction

The third most abundant species in Titan's atmosphere is molecular hydrogen, H_2. In the troposphere/tropopause region, Voyager IRIS measurements yielded an inferred H_2 mole fraction of 0.00112 ± 0.00016 (Samuelson et al., 1997) and 0.001 ± 0.0004 (Courtin et al., 1995). Cassini Composite Infrared Spectrometer (CIRS) measurements yield the same mixing ratio: 0.00096 ± 0.00024 southward of 40°N for the troposphere/tropopause region, with Courtin et al. (2008) basing their analysis on laboratory measurements of the collisionally induced H_2—N_2 dimer $S(0)$ transition at 355 cm^{-1}. Jennings et al. (2009) obtained an equatorial value of 0.001 ± 0.0005, from the $H_2S(1)$ line at 590 cm^{-1}, which samples the lower stratosphere at 70 km, and as Samuelson et al. (1997) based their analysis on ab initio collision-induced absorption models for H_2—N_2 collisions. Jennings et al. (2009) cite Courtin et al. (2008) that the winter northern polar value increases by a factor of 2, in the lower troposphere. This is an extremely remarkable variation, if real, because the H_2 lifetime is $\sim 8 \times 10^5$ year (e.g. Krasnopolsky, 2009) and hence should be well mixed horizontally. To date the Huygens Gas Chromatograph Mass Spectrometer (GCMS) team has not published a value for the H_2 mole fraction, but Niemann et al. (2010) in a talk on the Fifth Anniversary of the Huygens Landing did support the IRIS and CIRS results. At very high altitudes the INMS found the H_2 mixing ratio to be 0.00405 ± 0.0003 on the initial Titan flyby (Waite et al., 2005). From subsequent flybys Cui et al. (2008) constructed a globally averaged H_2 mole fraction profile in the thermosphere, which will be used in this study. Given the large separation distance (~1000 km) between these two independent measurements, the factor of ~4 difference would not seem significant except that H_2 tends to be essentially uniformly mixed throughout the atmosphere due to its long chemical lifetime and its enormous escape rate out of the atmosphere ($\sim 1 \times 10^{28}$ s^{-1}, Cui et al., 2008) which is essentially equal to, $\gtrapprox$99%, the maximum possible (limiting) rate (Strobel, 2009a).

Our current understanding of Titan's atmosphere is that hydrogen in atomic and molecular form results from the photochemical conversion of the much more abundant CH_4 into more complex, less saturated hydrocarbons with a net yield of hydrogen. Molecular hydrogen is, for all practical concerns, chemically inert in the atmosphere and production of H_2 is balanced by transport and eventual escape from the atmosphere, as implied by the INMS results (Yelle et al., 2006, 2008; Cui et al., 2008). This basic framework dates from the pre-Voyager model of Strobel (1974) to the comprehensive post-Voyager model of Yung et al. (1984), and Cassini epoch models of Wilson and Atreya (2004), Lavvas et al. (2008) and Krasnopolsky (2009). In spite of the increasing complexity of these models, the fact remains that H_2 is chemically inert, for example, Krasnopolsky (2009) finds that the integrated chemical loss of H_2 is only 2% of its integrated production rate. Furthermore, the small positive gradient in the H_2 mixing ratio inferred from the

* Fax: +1 410 516 7933.
E-mail address: strobel@jhu.edu

0019-1035/$ - see front matter © 2010 Elsevier Inc. All rights reserved.
doi:10.1016/j.icarus.2010.03.003

Please cite this article in press as: Strobel, D.F. Molecular hydrogen in Titan's atmosphere: Implications of the measured tropospheric and thermospheric mole fractions. Icarus (2010), doi:10.1016/j.icarus.2010.03.003

tropopause region to the lower thermosphere (~950–1000 km) and a satisfactory fit to the INMS profile in the thermosphere are not produced in any photochemical model to date. The purposes of this paper are to point out the extraordinary challenge this presents to modelers and that either the observations are not consistent with each other or that our understanding of CH_4 and H_2 photochemistry is flawed and needs some revision.

2. Equations and model

From the Huygens Probe's Atmospheric Structure Instrument (HASI), essentially continuous density, pressure, and temperature profiles are available for Titan's equatorial (10.3°S) atmosphere (Fulchignoni et al., 2005) and suitable for a 1D model. But comparison of the INMS densities with the HASI observations at equatorial latitudes near 1000 km altitude show INMS values to be ~2.4 times smaller than the HASI values. The Cassini Attitude and Articulation Control Subsystem (AACS) detects torques on the spacecraft as it enters Titan's upper atmosphere on each flyby, from which densities are derived that are, on average, about a factor of 2.6 larger than the INMS densities at 1000 km on the same trajectory and support the large HASI values (Müller-Wodarg et al., 2008; Strobel et al., 2009b). Accordingly, all INMS densities used in this study are increased by a factor of 2.6 as a function of altitude, but the mole fractions of CH_4 and H_2, in particular, remain unchanged at each altitude. As in a previous paper (Strobel, 2009a), the radial profiles of N_2, CH_4, H_2, Ar densities, kindly supplied by Drs. J. Cui (Cui et al., 2008) and I. Müller-Wodarg (Müller-Wodarg et al., 2008), represent globally averaged conditions based on flybys $T5$—$T43$. For N_2 and CH_4, these profiles are almost identical to what one would obtain by globally averaging the densities generated from Müller-Wodarg et al. (2008) empirical model for the northern hemisphere between altitudes 950 and 1600 km. Because our model is spherical 1D in the radial direction and represents globally averaged conditions, the appropriate comparison should be to globally averaged INMS densities.

For a multi component spherical 1D atmosphere, the individual conservation of momentum equations are (cf. Schunk and Nagy, 2000; Chapman and Cowling, 1970)

$$\frac{d(n_i kT)}{dr} + m_i n_i g = \sum_{j\neq i} m_i n_i \nu_{ij}(v_j - v_i) - \frac{1}{\sum_j n_j}\sum_{j\neq i} n_i n_j \alpha T_{ij}\frac{d(kT)}{dr} \quad (1)$$

$$= \sum_{j\neq i}\frac{n_i kT}{N_{ij}D_{ij}}\phi_j - \frac{kT}{D_i}\phi_i - \frac{1}{\sum_j n_j}\sum_{j\neq i} n_i n_j \alpha T_{ij}\frac{d(kT)}{dr} \quad (2)$$

where k is Boltzmann's constant, T is the atmospheric temperature, m_i is mass, g is the gravitational acceleration, r is radial distance, ν_{ij} are collision frequencies, $N_{ij}D_{ij}$ are mutual (binary) collision coefficients, $N_{ij} = n_i + n_j$, and D_i are the average diffusion coefficients defined as $D_i^{-1} = \sum_{j\neq i}\frac{n_j}{N_{ij}D_{ij}}$, ϕ_j are the fluxes $= n_j v_j$, αT_{ij} are the thermal diffusion factors. These equations are valid for small absolute and relative drift velocities in comparison to the thermal speeds, in essence low Mach number relative flows. Here it is assumed that the gases have a common temperature (cf. Appendix of Strobel (2009a)) and the values adopted for all coefficients are given in Strobel (2009a).

The input temperature profile needs to be sufficiently smooth in order to calculate accurate temperature gradients that are needed in Eq. (1). The HASI temperature profile is highly structured and contains ample evidence of waves. Because H_2 mole fraction data are limited to the troposphere and thermosphere above 950 km, the key requirement on the input temperature profile is that its average value is accurate enough to join the total tropospheric densities (mostly N_2) to the total thermospheric densities. In Fig. 1, two adopted temperature profiles are illustrated, which are analytic, infinitely differentiable, one with wave-like structures and the other without, and have average values over scale heights which allow the total model density profiles to match tropospheric and thermospheric measurements. All model cases were run with both temperature profiles, but results are shown for most cases with only the smooth, no waves, temperature profile, as the differences in the thermospheric density profiles and fluxes are insignificant. In Eq. (1) temperature dependencies associated with diffusion are very weak, $T/N_{ij}D_{ij} \propto\sim T^{0.25}$. For H_2, whose upward flux is essentially at the limiting rate, the limiting flux has the inverse, but same, weak temperature dependence, $N_{H_2,\,N_2}D_{H_2,\,N_2}/H_a \propto\sim T^{-0.25}$,

$$4\pi r^2\phi_l = 4\pi r^2 N_{H_2,N_2}D_{H_2,N_2}\mu_{H_2}\left[\frac{1}{H_a(r)} - \frac{1}{H_{H_2}(r)}\right] \sim 1\times 10^{28} H_2 s^{-1} \quad (3)$$

(cf. Hunten, 1973; Strobel, 2008), where subscript l denotes limiting, H_a, H_{H_2} are the scale heights of the background atmosphere and H_2, and μ_{H_2} is the H_2 mole fraction. With the adopted temperature profile, the calculated N_2 density profile joins smoothly with the INMS N_2 profile, as shown in Fig. 1.

The effects of eddy diffusion are incorporated in the continuity Eq. (4) in a manner identical to Strobel (2009a),

$$\frac{1}{4\pi r^2}\frac{d}{dr}\left[4\pi r^2\left(\phi_i - K_{zz}\left\{\frac{1}{T}\frac{d(n_i T)}{dr} + \frac{m_{N2}g}{kT}n_i\right\}\right)\right] = p_i - l_i \quad (4)$$

where ϕ_i is computed from the momentum Eq. (1), p_i and l_i are the globally averaged production and loss rates ($cm^{-3}\,s^{-1}$), and the eddy diffusion coefficient, $K_{zz}(r)$, is constrained by the INMS Ar density profile supplied by Cui et al. (2009). Because the large upward CH_4 and H_2 fluxes render these species insensitive to eddy diffusion, the determination of the homopause location, where eddy and Ar molecular diffusion coefficients are equal, is specific to Ar only and located at approximately 855 km. The $K_{zz}(r)$ profile shape is given in Fig. 6 of Strobel (2009a), but note that the INMS densities in this paper are 2.6 times those in Strobel (2009a).

Throughout most of the atmosphere CH_4 is being irreversibly dissociated by direct photolysis driven principally by the intense solar Lyman α line at 121.6 nm, indirectly by catalytic C_2H_2 photochemistry, and by ion chemistry with net production of H_2, H, and heavy hydrocarbons. Overall, the most abundant photolysis product is C_2H_6, followed by C_2H_2 (although not in all models, e.g. Lavvas et al. (2008) find C_3H_8 next most abundant). The chemistry that is required for this study is to get the local production of H_2, p_{H_2}, approximately correct in Eq. (4) and its height integrated production more accurate. Similar requirements are necessary for the loss of CH_4, l_{CH4}, in Eq. (4). While one could tackle this problem with a comprehensive model such as those of Yung et al. (1984), Wilson and Atreya (2004), Lavvas et al. (2008), and Krasnopolsky (2009), this would be overkill given the long chemical lifetimes of CH_4 and H_2; due, for the former, that most dissociation is irreversible and, for the latter, that chemical loss is negligible. Instead, the following chemical model is adopted:

$$\text{Ionospheric photolysis}: 2CH_4 \rightarrow C_2H_2 + 3H_2 \quad (5)$$

$$\text{Direct photolysis}: 2CH_4 \rightarrow C_2H_4 + 2H_2 \quad (6)$$

$$\text{Catalytic photolysis}: 2CH_4 \rightarrow C_2H_6 + H_2 \quad (7)$$

In Strobel (2009a), ionospheric chemistry was modeled simply by $2CH_4 \rightarrow C_2H_4 + H_2 + 2H$, whereas here it is assumed that some CH_4 gets converted to very complex positive and negative ions, deficient in hydrogen, and eventually aerosol monomers after recombination. The basis for this assumption is the numerous Cassini measurements of positive ions (Cravens et al., 2006; Vuitton et al., 2007), negative ions (Coates et al., 2007; Vuitton et al., 2009), and aerosol formation (Waite et al., 2007; Lavvas et al.,

Please cite this article in press as: Strobel, D.F. Molecular hydrogen in Titan's atmosphere: Implications of the measured tropospheric and thermospheric mole fractions. Icarus (2010), doi:10.1016/j.icarus.2010.03.003

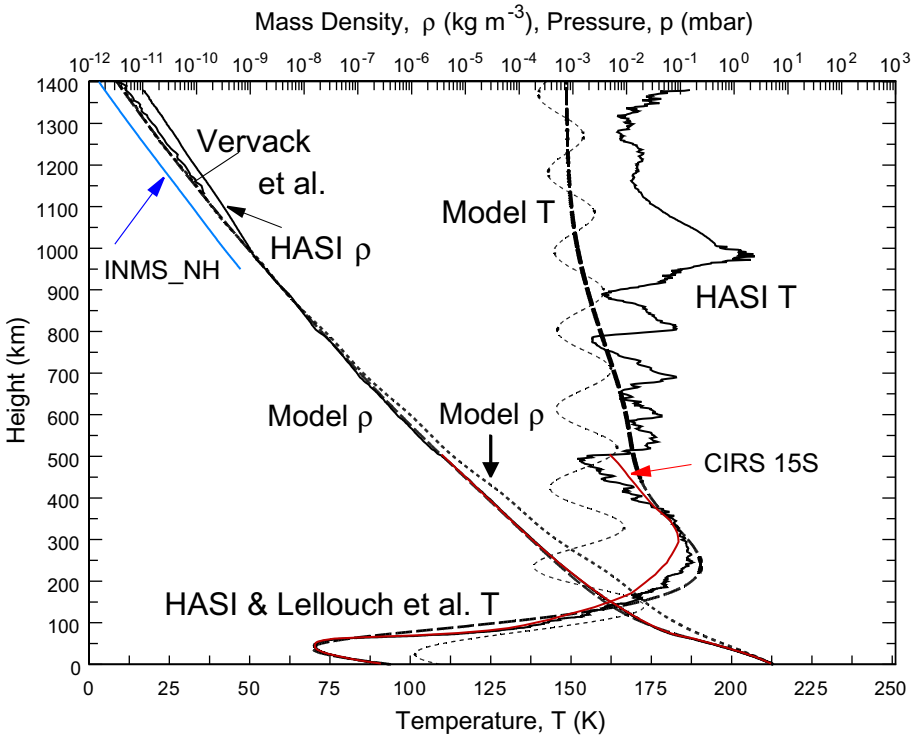

Fig. 1. Model atmospheres with and without waves compared to Voyager data (Lellouch et al., 1989; Vervack et al., 2004) and Cassini-Huygens data (Fulchignoni et al., 2005; Müller-Wodarg et al., 2008; Vinatier et al., 2007). Note that the INMS data have not been increased by a factor of 2.6 in this figure.

2009; Wahlund et al., 2009). The latter authors estimate an ionospheric aerosol formation rate of $\sim 3 \times 10^{-15}$ g cm^{-2} s^{-1}, whereas Lavvas et al. (2009) obtained $(2.7–4.6) \times 10^{-14}$ g cm^{-2} s^{-1} above $z = 500$ km, all referenced to the surface. For the direct photolysis model, the only important aspect is that $1CH_4$ molecule produces $1H_2$ molecule. The dominant photolysis path is the indirect, catalytic one and the principal product is C_2H_6 to be consistent with observations. In Fig. 2, these photolytic paths are shown, centered at 3700, 3400, and 2800 km, respectively. The diurnally, globally averaged irreversibly CH_4 loss rate is 1.5×10^{10} cm^{-2} s^{-1} and the corresponding production rate for H_2 is 1.1×10^{10} cm^{-2} s^{-1}. Note that these rates are all r^2 weighted and referenced to Titan's surface. The CH_4 loss rate compares favorably with the rates of Yung et al. (1984): 1.5×10^{10}, Wilson and Atreya (2004): 8.7×10^{9},

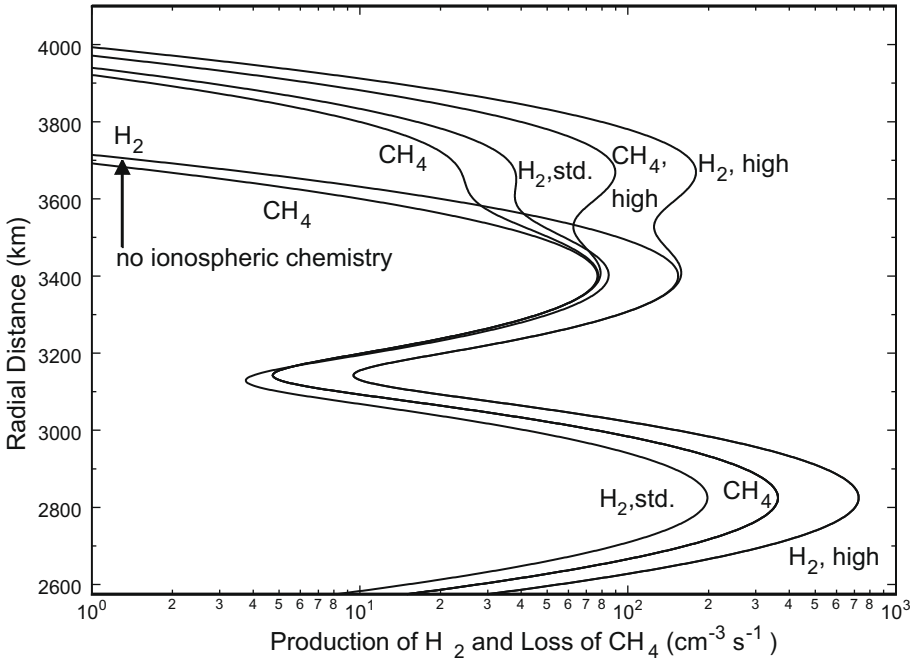

Fig. 2. Specified CH_4 and H_2 loss and production rates, respectively, for standard assumptions and for high ionization rate + extreme stoichiometric equation: $2CH_4 \rightarrow C_2 + 4H_2$.

Please cite this article in press as: Strobel, D.F. Molecular hydrogen in Titan's atmosphere: Implications of the measured tropospheric and thermospheric mole fractions. Icarus (2010), doi:10.1016/j.icarus.2010.03.003

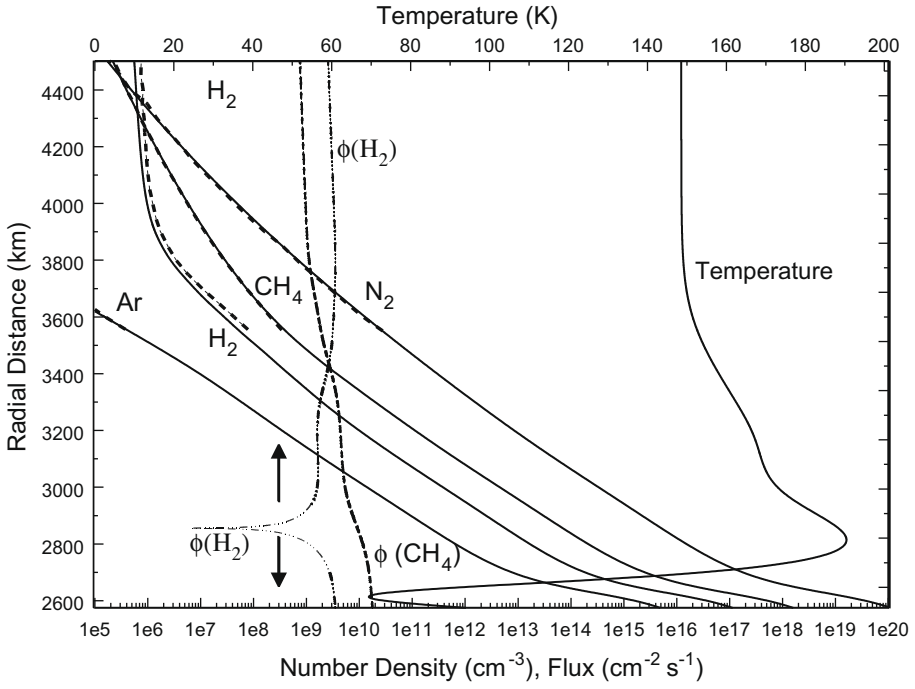

Fig. 3. The standard model for Titan's atmosphere with CIRS lower boundary condition for H_2 mole fraction. Calculated density profiles (solid lines), INMS density profiles (dashed lines), CH_4 flux is positive and upward, arrows indicate direction of H_2 flux, see text for temperature profile.

Lavvas et al. (2008): 1.3×10^{10} and Krasnopolsky (2009): 9.4×10^9 cm^{-2} s^{-1}. For the corresponding production rates of H_2 (equal to the escape flux) the comparison is less favorable (Yung et al. (1984): 1.0×10^{10}, Wilson and Atreya (2004): 6.5×10^9, and Lavvas et al. (2008): 4.7×10^9 cm^{-2} s^{-1}, where the rates are for $H_2 + 1/2H$ and Krasnopolsky (2009): 1.2×10^{10} cm^{-2} s^{-1}). But note that the former two, pre-Cassini papers assumed that Jeans escape was the mechanism driving H_2 escape, whereas analyses of INMS data yield escape fluxes of 1.4×10^{10} (Cui et al., 2008), and $1.1 \times 10^{10}$$H_2$ cm^{-2} s^{-1} (Strobel, 2009a), in much better agreement.

For N_2 and Ar, $p = l = 0$, as at most only a small fraction of N_2 molecules that are ionized and dissociated are not recycled back to N_2, but become nitriles such as *HCN* and diffuse out of the ionosphere. Argon is for our purposes inert. Eqs. (1) and (4) are equations for $\frac{dn_i}{dr}$ and $\frac{d\phi_i}{dr}$, respectively, that are solved numerically with a fourth-order Runge–Kutta algorithm and step size of 1 km, where all boundary conditions are applied at Titan's surface. At the surface the HASI total density is 1.14×10^{20} cm^{-3} (Fulchignoni et al., 2005), the CH_4 mole fraction is set to 0.014, its stratospheric value although it is close to 0.05 at the surface, but then decreases to

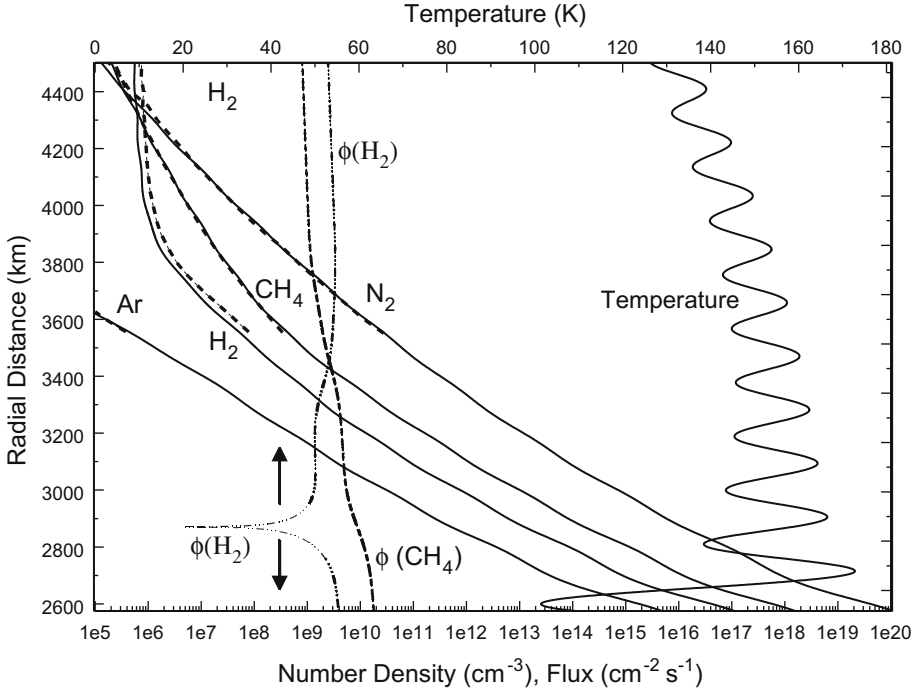

Fig. 4. The standard model for Titan's atmosphere with CIRS lower boundary condition for H_2 mole fraction. Calculated density profiles (solid lines), INMS density profiles (dashed lines), CH_4 flux is positive and upward, arrows indicate direction of H_2 flux, see text for temperature profile.

Please cite this article in press as: Strobel, D.F. Molecular hydrogen in Titan's atmosphere: Implications of the measured tropospheric and thermospheric mole fractions. Icarus (2010), doi:10.1016/j.icarus.2010.03.003

0.016 by 32 km (Niemann et al., 2005); the H_2 mole fraction is set to 0.001 (Courtin et al., 1995, 2008; Samuelson et al., 1997) and the Ar mole fraction is 4.32×10^{-5} (Niemann et al., 2005). The CH_4 condensation cycle in the lower troposphere is omitted, because it does not impact our results. The fluxes of CH_4 and H_2 at the lower boundary are adjusted until suitable fits to their INMS profiles in the thermosphere are achieved. The N_2 and Ar fluxes are set to zero. The escape fluxes in this paper are calculated at the exobase, $r = 4100$ km, altitude equal to 1525 km, and referenced to the surface. Note that the model is integrated upwards from the lower boundary, where densities and fluxes are specified, and can be terminated at any level in the atmosphere without impacting the calculated densities and fluxes below this level.

3. Results

Our standard solution and input temperature profile (no waves) are illustrated in Fig. 3, with the CIRS lower boundary condition of 0.001 for the H_2 mole fraction. This calculation does not yield an acceptable fit to the INMS H_2 density profile and, in fact, is ~0.65 times the INMS values. The basic choices are to get H_2 density/mole fraction correct at $r = 3600$ km, or to get the correct shape of the density/mole fraction profile, but underpredict their absolute values. For this case, Titan's interior must supply the atmosphere with $1.5 \times 10^{28} CH_4\ s^{-1}$, in steady state, of which $1.9 \times 10^{27} CH_4\ s^{-1}$ escape from the atmosphere, whereas $2.9 \times 10^{27} H_2\ s^{-1}$ flow into the surface and $6.6 \times 10^{27} H_2\ s^{-1}$ escape Titan. To confirm that our solutions are largely independent of the detailed structure of the input temperature profile, Fig. 4 displays the same case, but with the other temperature profile. In this case there are slight differences in the fluxes. Titan's interior must still supply the atmosphere $1.5 \times 10^{28} CH_4\ s^{-1}$, of which $2.0 \times 10^{27} CH_4\ s^{-1}$ escape from the atmosphere, whereas $3.2 \times 10^{27} H_2\ s^{-1}$ flow into the surface and $6.3 \times 10^{27} H_2\ s^{-1}$ escape Titan. The H_2 flow into the surface is demanded by the fact that INMS H_2 mole fraction in the thermosphere exceeds the CIRS inferred mole fraction in the troposphere by $\gtrsim 2$. To illustrate this, the lower boundary condition of 0.001 for the H_2 mole fraction was increased to 0.0022 and the new profiles are shown in Fig. 5. The INMS density profiles are now well reproduced with escape rates of $1.9 \times 10^{27} CH_4\ s^{-1}$ and $9.6 \times 10^{27} H_2\ s^{-1}$, essentially the solution in Fig. 6 of Strobel (2009a). At the surface as before, Titan's interior must supply the atmosphere $1.5 \times 10^{28} CH_4\ s^{-1}$, whereas now only $1.8 \times 10^{26}\ H_2\ s^{-1}$ flow into of the surface. But compared to the H_2 escape rate and the integrated H_2 production rate of $9.6 \times 10^{27} H_2\ s^{-1}$, this flux is not numerically significant and, in fact, a slight decrease in the production rate could reduce the calculated H_2 flux at the surface to precisely 0.

In order to illustrate how difficult it is to explain the altitude variation of the H_2 mole fraction, extreme assumptions are made about atmospheric photochemistry. Instead of the chemical scheme represented by Eqs. (5)–(7), the product for each of these stoichiometric equations is now: $2CH_4 \rightarrow C_2 + 4H_2$. In addition, the ionospheric ionization rate was increased by a factor of four, as evident by increased ionospheric loss rate of CH_4 (labeled CH_4 *high*) and the increased ionospheric production rate of H_2 (labeled H_2 *high*) shown in Fig. 2. For H_2 there is the additional increase due to the assumption that four, rather than three, H_2 are produced at the expense of $2CH_4$. Thus the overall integrated production rate of H_2 is increased by a factor of ~3.4, whereas the overall integrated loss rate of CH_4 increases slightly from $1.5 \times 10^{10}\ cm^{-2}\ s^{-1}$ to $1.9 \times 10^{10}\ cm^{-2}\ s^{-1}$. The results of this numerical experiment are given in Fig. 6, where it is shown that this large increase in the H_2 production, particularly at ionospheric heights, yields the observed INMS H_2 density profile with the CIRS H_2 mole fraction lower boundary condition of 0.001. The calculated thermospheric H_2 density profile is strongly affected by ionospheric chemistry and consequently, a precise fit of the INMS data was not possible for a unique value of its escape flux. Here the H_2 escape rate is $1.5 \times 10^{28} H_2\ s^{-1}$ and to balance the integrated production rate there is a $1.6 \times 10^{28} H_2\ s^{-1}$ flowing into the surface. The large ionospheric loss rate imposes chemical, rather than diffusive, control on CH_4 in the ionosphere and requires an influx of 4.1×10^{26}

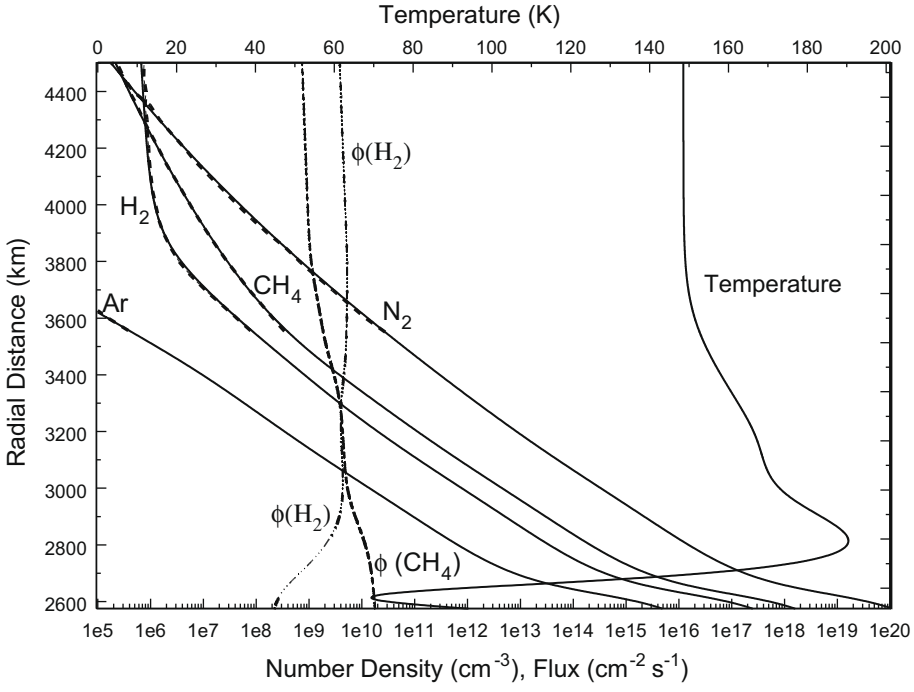

Fig. 5. Same as Fig. 3, but with lower boundary condition for H_2 mole fraction 2.2 times CIRS value. All fluxes are upward.

Please cite this article in press as: Strobel, D.F. Molecular hydrogen in Titan's atmosphere: Implications of the measured tropospheric and thermospheric mole fractions. Icarus (2010), doi:10.1016/j.icarus.2010.03.003

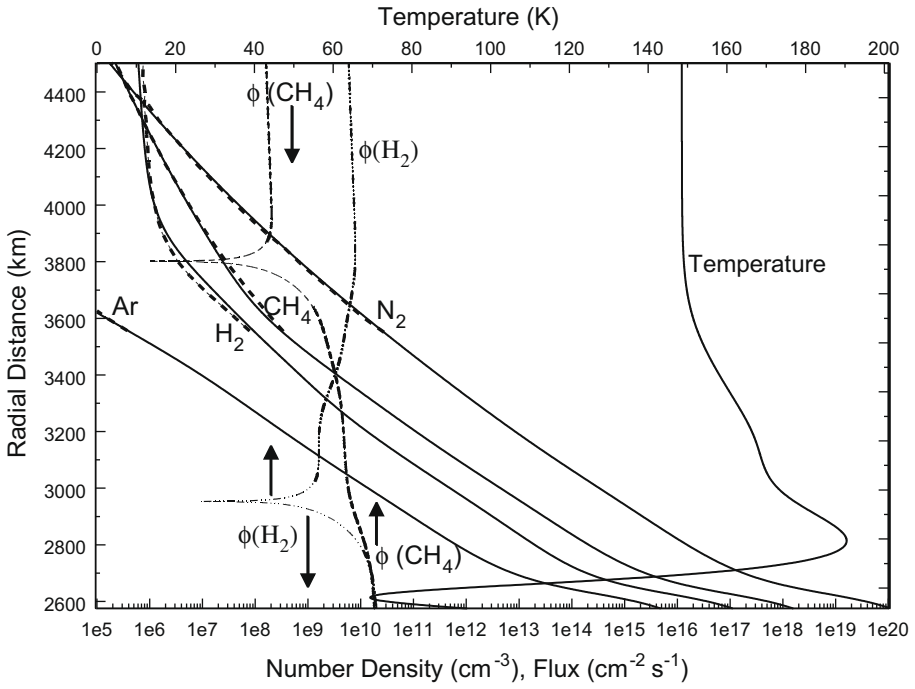

Fig. 6. Same as Fig. 3, but with high ionization rate + extreme stoichiometric equation: $2CH_4 \rightarrow C_2 + 4H_2$. Direction of fluxes are indicated by arrows.

$CH_4\ s^{-1}$, which is essentially zero in comparison to surface outflow of $1.5 \times 10^{28} CH_4\ s^{-1}$. This is one potential way to satisfy the observational values of the H_2 mole fraction, and to render the CH_4 escape rate negligibly small, if there were a power source(s) large enough to support the enhance ionization.

To judge the impact of the large ionospheric rates in this calculation, the calculation was repeated with the ionospheric rates for CH_4 and H_2 set to zero, as illustrated in Fig. 2, but still with the assumption that $2CH_4 \rightarrow C_2 + 4H_2$, everywhere. The results of this calculation are shown in Fig. 7, where a slight compromise was made to fit the shape of the INMS H_2 density profile. This compromise leads to an insignificant 10% underestimate of the H_2 density at 3600 km and an H_2 escape rate of $7.7 \times 10^{27} H_2\ s^{-1}$, which is essentially equal to the limiting rate. It is also interesting that most of the increased H_2 production is balanced by a larger downward flux into the surface (compare $1.6 \times 10^{28} H_2\ s^{-1}$, Fig. 7; with $2.9 \times 10^{27} H_2\ s^{-1}$, Fig. 3) with an insignificant increase in the H_2 escape rate. This large downward H_2 flow rate into Titan's surface is

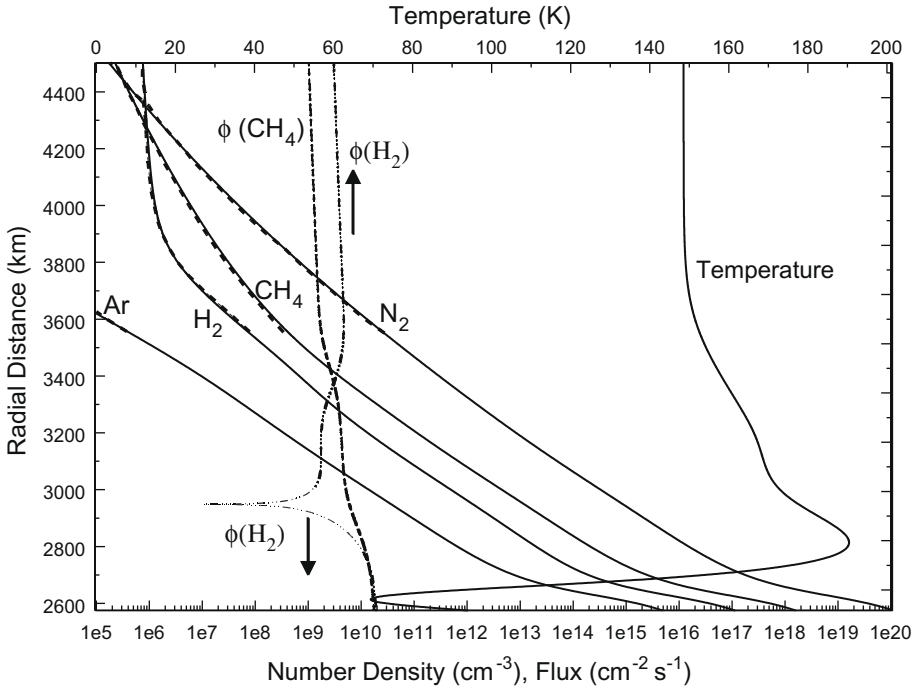

Fig. 7. Same as Fig. 6, but with high ionization rate set to zero, CH_4 flux is positive and upward, arrows indicate direction of H_2 flux.

Please cite this article in press as: Strobel, D.F. Molecular hydrogen in Titan's atmosphere: Implications of the measured tropospheric and thermospheric mole fractions. Icarus (2010), doi:10.1016/j.icarus.2010.03.003

required to fit the reported CIRS and INMS measurements. In the absence of ionospheric loss, $2.6 \times 10^{27} CH_4\ s^{-1}$ escape from the atmosphere, which is consistent with Yelle et al. (2008), who did not include ionospheric loss.

However, there is no laboratory nor observational support for the extreme assumption that $2CH_4 \rightarrow C_2 + 4H_2$, as the dominant product of CH_4 photolysis is C_2H_6. Furthermore, the integrated, r^2 weighted and referenced to Titan's surface, ionization rate for the high rate case is $3.8 \times 10^9\ cm^{-2}\ s^{-1}$, corresponding to a peak electron density of $8000\ cm^{-3}$, at least a factor of 2 times radio occultation measurements (Kliore et al., 2008), and with an effective recombination coefficient of $\alpha_{rec} = 10^{-6}\ cm^3\ s^{-1}$ (cf. Galand et al., 1999). This integrated ionization rate is an order of magnitude larger than computed by Wilson and Atreya (2004) and Krasnopolsky (2009). Accordingly, neither the enhanced ionization rate nor extreme stripping of hydrogen from CH_4 are viable solutions.

Since there is no apparent chemical solution to satisfy simultaneously the observed H_2 mole fractions in the troposphere and thermosphere, a possible solution is explored by modification of diffusive transport in Eqs. (1) and (4). The observational fact that the H_2 mole fraction increases with altitude implies that eddy diffusion drives a downward flux, whereas molecular diffusion drives an upper flux. According to the results of Fig. 3, the eddy diffusion flux exceeds the molecular diffusion flux below $r = 2850$ km and vice versa above this altitude. Clearly this transition level can be decreased in altitude by reduction in the magnitude of the eddy diffusion coefficient, K_{zz}. Also, in the molecular diffusion dominated region the solution to Eqs. (1) and (4) contains two basic terms: (1) a solution that corresponds to the limiting flux (cf. Eq. (3) solved for μ_{H_2}) and (2) a static solution that corresponds to gravitational diffusive equilibrium, where $n_{H_2}(r) \propto \exp\left(-\int dr/H_{H_2}\right)$, and $H_{H_2} = \left(\frac{m_{H_2} g}{kT} + \frac{1}{T}\frac{dT}{dr}\right)^{-1}$ is the H_2 density scale height. A suitable linear combination of these two terms in an atmosphere dominated by molecular diffusion can satisfy the CIRS and INMS measurements. In Fig. 8 the eddy diffusion coefficient was set to $K_{zz} = 100\ cm^2\ s^{-1}$ for H_2 and unaltered for all other species. When compared to Fig. 3, the solutions for N_2, CH_4, Ar densities are essentially identical. But now the calculated H_2 density at 3600 km exceeds the INMS density by ~20%, $1.7 \times 10^{27} H_2\ s^{-1}$ flow out of the surface (in contrast to Fig. 3, where $2.9 \times 10^{27} H_2\ s^{-1}$ flow into the surface) and $1.1 \times 10^{28} H_2\ s^{-1}$ escape Titan. Because the former is only 15% of the latter, fine tuning of the H_2 production rate and K_{zz} could render the surface flow essentially zero.

Of course, it is difficult to justify that only H_2 could be subject to low eddy mixing in the atmosphere. To explore the impact of low eddy mixing for all constituents, a run with $K_{zz} = 150\ cm^2\ s^{-1}$ was made and illustrated in Fig. 9. Note that the density profiles for N_2, H_2 are identical, with one small exception, a slightly lower rate of $1.4 \times 10^{27} H_2\ s^{-1}$ flow out of the surface. Further increases in the magnitude of K_{zz} would eventually yield a solution with zero H_2 flux at the surface, as the standard run in Fig. 3 has $2.9 \times 10^{27} H_2\ s^{-1}$ flowing into the surface. As expected, without vigorous eddy mixing in the atmosphere, the density profile of inert, heavier than N_2, Ar cannot be calculated correctly in a spherical 1D model. Although CH_4, like H_2, is lighter than N_2, it is not chemically inert and in the ~3300–3500 km region, where it is subject to direct photolysis, chemistry is competitive with molecular diffusion, and in the absence of eddy diffusion, causes the actual CH_4 scale height to be smaller than the expected N_2 scale height for near limiting flux conditions. The implication from Fig. 9 is that one cannot argue that light species ($m < m_{N_2}$) should have much lower values of K_{zz} than heavier ones.

4. Concluding remarks

There is no apparent solution that satisfies the two observational constraints on the H_2 mole fraction: (1) in the troposphere and lower stratosphere from the IR measurements of Voyager IRIS and Cassini CIRS of 0.001 and (2) the Cassini INMS measurements in the thermosphere above 3525 km. The infrared experiments on Voyager and Cassini have consistently converged on the tropospheric H_2 mole fraction to be 0.001 (Courtin et al., 1995, 2008; Samuelson et al., 1997; although Samuelson et al. (1981) initially derived 0.002 ± 0.001). The $H_2 S(0)$ probes the lower troposphere at ~10 km, whereas the $S(1)$ samples the lower stratosphere at ~70 km, and no gradient in the H_2 mole fraction between these two regions has been reported or expected. These analyses are based on both laboratory measurements of the collisionally induced H_2–N_2 dimer $S(0)$ transition at $355\ cm^{-1}$, and for the H_2 $S(1)$ line at $590\ cm^{-1}$, ab initio collision-induced absorption models with a stated accuracy of ±10–15%, when normalized to laboratory measurements in the temperature range: 90–300 K (Samuelson et al., 1997). The confirmation of the IR results by Niemann et al. (2010), coupled with the long lifetime of H_2 in the atmosphere, validates that the near surface H_2 mole fraction is 0.001 with an uncertainty of ~25%. Note that Courtin et al. (2008) find this value applies over the region 40°N to the south pole and hence is effectively the globally averaged magnitude.

While the absolute measured values of densities by INMS are apparently a factor of ~2.6 lower than densities measured by HASI and inferred from torques by the Cassini AACS, it is not expected that the ratios of densities, in particular, the H_2/N_2 ratio, is uncertain by more than approximately 20% and certainly not a factor of 2. Without any adjustment in either or both the CIRS and INMS H_2 mole fractions, they jointly require a downward flux of H_2 into Titan's surface at a rate on the order of $10^{28} H_2\ s^{-1}$, comparable to the H_2 escape rate.

Given the irreversible nature of CH_4 photochemistry and the deposition of less saturated, more complex hydrocarbons and organic molecules on Titan's surface (cf. Lorenz et al. (2008), for an inventory of these substances), it is certainly possible that these hydrocarbons could recombined with H_2 to reform CH_4 as recombination would be an exothermic process in contrast to the endothermic decomposition of CH_4. The reaction rates would be extremely slow at surface temperatures as one would expect an energy barrier analogous to an activation energy for recombination to occur, unless catalytic element or minerals are available on Titan's surface to mitigate the energy barrier, the reaction rates would be extremely slow at surface temperatures. In fact, McKay and Smith (2005) discuss this possibility in the speculative context of methanogenic life on Titan. They state "If life is consuming atmospheric hydrogen it will have a measurable effect on the hydrogen mixing ratio in the troposphere if the biological consumption is greater than $10^8\ cm^{-2}\ s^{-1}$". From the calculations in Figs. 6 and 7, the Cassini-Huygens H_2 measurements imply that the downward H_2 surface flux is $\sim 2 \times 10^{10}\ cm^{-2}\ s^{-1}$, in substantial excess of their threshold value, but unlike their calculations the surface H_2 mole fraction is 0.001 in contrast to their off-scale value of much less than 10^{-5}.

It should be emphasized that in spite of the implication that large downward H_2 surface fluxes are demanded by the data and may imply reversible CH_4 chemistry on or below the surface, the large H_2 escape rates inferred from INMS data still require irreversible CH_4 photochemistry in the atmosphere. The large downward H_2 surface fluxes are not as surprising as the additional, factor of ~2, increased CH_4 destruction rate in the atmosphere than accounted for by previous and current photochemical models, as the model assumption that $2\ CH_4 \rightarrow C_2 + 4H_2$, everywhere, is not

Please cite this article in press as: Strobel, D.F. Molecular hydrogen in Titan's atmosphere: Implications of the measured tropospheric and thermospheric mole fractions. Icarus (2010), doi:10.1016/j.icarus.2010.03.003

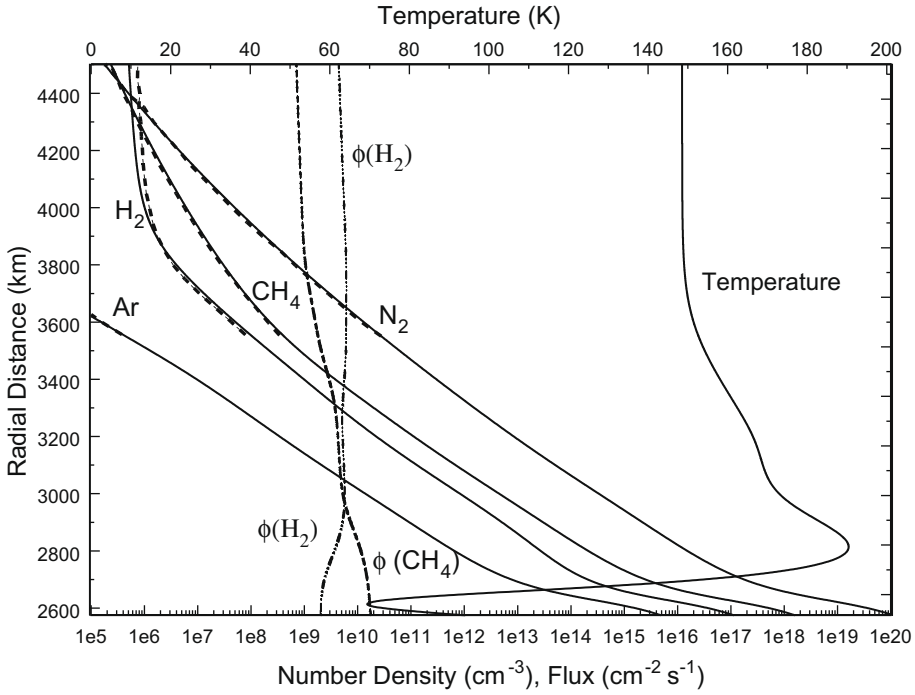

Fig. 8. Same as Fig. 3, but with low $K_{zz} = 100\ cm^2\ s^{-1}$ for H_2 only, all fluxes are upward.

viable. The author is not aware of any evidence from Cassini spacecraft instruments that Saturn's magnetospheric interaction with Titan's upper atmosphere plays a major role in the integrated CH_4 chemical loss. The most obvious solution to enhanced photochemical destruction of CH_4 is higher efficiencies from the catalytic reactions associated with photolysis of C_2H_2 and other polyacetylenes.

Finally in this spherical 1D model transport is necessarily diffusive. Because the constant H_2 mixing ratio surfaces increase with altitude, a meridional circulation would tilt these mixing ratio surfaces in the following sense (cf. Holton and Schoeberl, 1988; Bacmeister et al., 1995). Downward motion (subsidence) brings down higher mixing ratios from above while upward motion brings lower mixing ratios from below. Hence enrichment with latitude in the Northern Hemisphere as found by Courtin et al. (2008) in the troposphere implies subsidence over Titan's North Pole in the winter season during the Cassini Nominal Mission and consistent with the conclusions of Teanby et al. (2008) from chemical tracers in the winter, northern polar vortex of Titan's stratosphere.

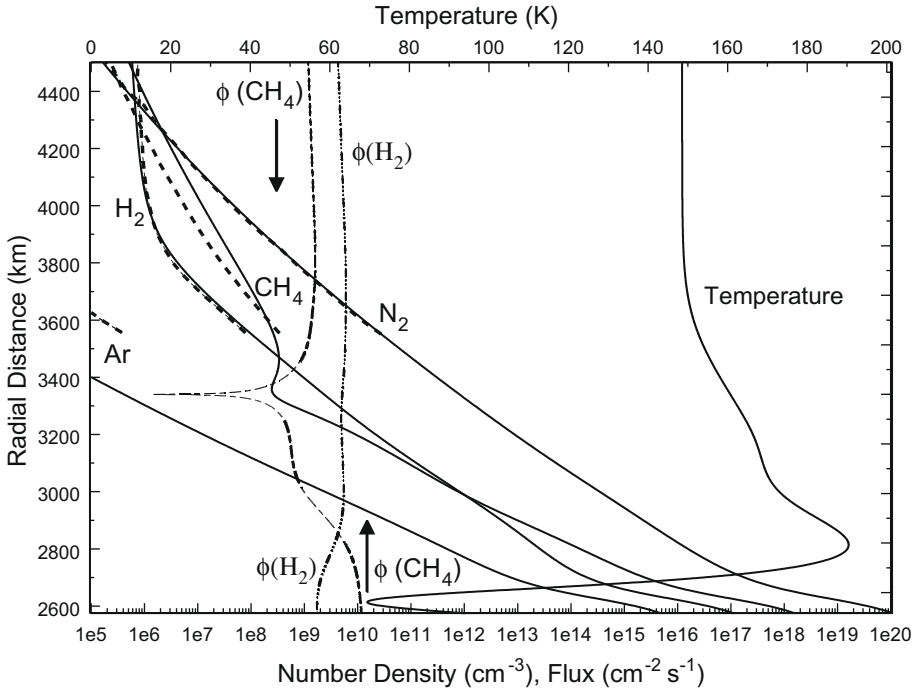

Fig. 9. Same as Fig. 8, but with low $K_{zz} = 150\ cm^2\ s^{-1}$ for all species, H_2 flux is positive and upward, arrows indicate direction of CH_4 flux.

Please cite this article in press as: Strobel, D.F. Molecular hydrogen in Titan's atmosphere: Implications of the measured tropospheric and thermospheric mole fractions. Icarus (2010), doi:10.1016/j.icarus.2010.03.003

Given the long chemical and residence times of H_2 in the atmosphere, the meridional circulation would produce a net downward transport of H_2 to the surface due to the H_2 positive mole fraction gradient and conservation of mass.

Acknowledgments

This research was supported by the Cassini-Huygens Mission through JPL Contract Nos. 1353551 and NASA Grant NNG05GO91G. The author thanks Drs. Müller-Wodarg and Cui for the digital INMS data used in Figs. 1, 3–9, and the referees for their helpful comments.

References

Bacmeister, J.T., Schoeberl, M.R., Summers, M.E., Rosenfield, J.R., Zhu, X., 1995. Descent of long-lived trace gases in the winter polar vortex. J. Geophys. Res. 100, 11669–11684.

Chapman, S., Cowling, T.G., 1970. The Mathematical Theory of Non-Uniform Gases, third ed. Cambridge University Press, Cambridge. 423 pp. (Chapter 18).

Coates, A.J., Crary, F.J., Lewis, G.R., Young, D.T., Waite Jr., J.H., Sittler Jr., E.C., 2007. Discovery of heavy negative ions in Titan's ionosphere. Geophys. Res. Lett. 34, L22103. doi:10.1029/2007GL030978.

Cravens, T.E., Robertson, I.P., Waite Jr., J.H., 2006. The composition of Titan's ionosphere. Geophys. Res. Lett. 33, L07105. doi:10.1029/2005GL025575.

Courtin, R., Gautier, D., McKay, C.P., 1995. Titan's thermal emission spectrum: Reanalysis of the Voyager infrared measurements. Icarus 114, 114–162.

Courtin, R.D., Sim, C., Kim, S., Gautier, D., Jennings, D.E., 2008. Latitudinal variations of tropospheric H_2 on Titan from the Cassini CIRS investigation [40th DPS Meeting Abstract. 31.01, Ithaca, New York]. Bull. Am. Astron. Soc. 40 (31.01), 446.

Cui, J., Yelle, R.V., Volk, K., 2008. Distribution and escape of molecular hydrogen in Titan's thermosphere and exosphere. J. Geophys. Res. 113, E10004. doi:10.1029/2007JE003032.

Cui, J., and 12 colleagues, 2009. Analysis of Titan's neutral upper atmosphere from Cassini Ion Neutral Mass Spectrometer measurements. Icarus. doi:10.1016/j.icarus.2008.12.

Fulchignoni, M., and 42 colleagues, 2005. Titan's physical characteristics measured by the Huygens Atmospheric Structure Instrument (HASI). Nature 438, 785–791. doi:10.1038/nature04314.

Galand, M., Lilensten, J., Toublanc, D., Maurice, S., 1999. The ionosphere of Titan: Ideal diurnal and nocturnal cases. Icarus 140, 92–105.

Holton, J.R., Schoeberl, M.R., 1988. The role of gravity wave generated advection and diffusion in transport of tracers in the mesosphere. J. Geophys. Res. 93, 11075–11082.

Hunten, D.M., 1973. The escape of light gases from planetary atmospheres. J. Atmos. Sci. 30, 1481–1494.

Jennings, D.E., and 19 colleagues, 2009. Titan's surface brightness temperatures. Astrophys. J. 691, L103–L105. doi:10.1088/0004-637X/691/2/L103.

Kliore, A.J., and 12 colleagues, 2008. First results from the Cassini radio occultations of the Titan ionosphere. J. Geophys. Res. 113, A09317. doi:10.1029/2007JA012965.

Krasnopolsky, V.A., 2009. A photochemical model of Titan's atmosphere and ionosphere. Icarus 201, 226–256. doi:10.1016/j.icarus.2008.12.038.

Lavvas, P.P., Coustenis, A., Vardavas, I.M., 2008. Coupling photochemistry with haze formation in Titan's atmosphere, part II: Results and validation with Cassini/Huygens data. Planet. Space Sci. 56, 67–99.

Lavvas, P.P., Yelle, R.V., Vuitton, V., 2009. The detached haze layer in Titan's mesosphere. Icarus. doi:10.1016/j.icarus.2009.01.004.

Lellouch, E., Coustenis, A., Gautier, D., Raulin, F., Dubouloz, N., Frere, C., 1989. Titan's atmosphere and hypothesized ocean: A reanalysis of the Voyager 1 radio occultation and IRIS 7.7 μm data. Icarus 79, 328–349.

Lorenz, R.D., and 15 colleagues, 2008. Titan's inventory of organic surface materials. Geophys. Res. Lett. 35, L02206. doi:10.1029/2007GL032118.

McKay, C.P., Smith, H.D., 2005. Possibilities for methanogenic life in liquid methane on the surface of Titan. Icarus 178, 274–276. doi:10.1016/j.icarus.2005.05.018.

Müller-Wodarg, I.C.F., Yelle, R.V., Cui, J., Waite Jr., J.H., 2008. Horizontal structures and dynamics of Titan's thermosphere. J. Geophys. Res. 113, E10005. doi:10.1029/2007JE003033.

Niemann, H.B., and 17 colleagues, 2005. The abundances of constituents of Titan's atmosphere from the GCMS instrument on the Huygens probe. Nature 308, 779–784. doi:10.1038/nature04122.

Niemann, H.B., and the GCMS Team, 2010. GCMS, Cassini-Huygens Project: Huygens Legacy and Future Titan Exploration Meeting at CosmoCaixa, Barcelona, January 13–15.

Samuelson, R.E., Hanel, R.A., Kunde, V.G., Maguire, W.C., 1981. Mean molecular weight and hydrogen abundance of Titan's atmosphere. Nature 292, 688–693.

Samuelson, R.E., Nath, N.R., Borysow, A., 1997. Gaseous abundances and methane supersaturation in Titan's troposphere. Planet. Space Sci. 45, 959–980.

Schunk, R.W., Nagy, A.F., 2000. Ionospheres – Physics, Plasma Physics, and Chemistry. Cambridge University Press, Cambridge, UK. 554 pp..

Strobel, D.F., 1974. The photochemistry of hydrocarbons in the atmosphere of Titan. Icarus 21, 466–470.

Strobel, D.F., 2008. Titan's hydrodynamically escaping atmosphere. Icarus 193, 588–594. doi:10.1016/j.icarus.2007.08.014.

Strobel, D.F., 2009a. Titan's hydrodynamically escaping atmosphere: Escape rates and the structure of the exobase region. Icarus 202, 632–641. doi:10.1016/j.icarus.2009.03.007.

Strobel, D.F., Atreya, S.K., Bézard, B., Ferri, F., Flasar, F.M., Fulchignoni, M., Lellouch, E., Müller-Wodarg, I.C.F., 2009b. Atmospheric structure and composition. In: Brown, R.H., Lebreton, J.-P., Waite, J.H., Jr. (Eds.), Titan from Cassini-Huygens. Springer, pp. 235–257. doi:10.1007/978-1-4020-9215-2.

Teanby, N.A., and 12 colleagues, 2008. Titan's polar vortex structure revealed by chemical tracers. J. Geophys. Res. 113, E12003. doi:10.1029/2008JE003218.

Vervack Jr., R.J., Sandel, B.R., Strobel, D.F., 2004. New perspectives on Titan's upper atmosphere from a reanalysis of the Voyager 1 UVS solar occultations. Icarus 170, 91–112.

Vinatier, S., and 10 colleagues, 2007. Vertical abundance profiles of hydrocarbons in Titan's atmosphere at 15°S and 80°N retrieved from Cassini/CIRS spectra. Icarus 188, 120–138.

Vuitton, V., Yelle, R.V., McEwan, M.J., 2007. Ion chemistry and N-containing molecules in Titan's upper atmosphere. Icarus 191, 722–742. doi:10.1016/j.pss.2009.04.004.

Vuitton, V., Lavvas, P., Yelle, R.V., Galand, M., Wellbrock, A., Lewis, G.R.,Coates, A.J., Wahlund, J.-E., 2009. Negative ion chemistry in Titan's upper atmosphere. Planet. Space Sci., in press. doi:10.1016/j.pss.2009.04.004.

Wahlund, J.-E., and 18 colleagues, 2009. On the amount of heavy molecular ions in Titan's ionosphere. Planet. Space Sci. doi:10.1016/j.pss.2009.07.014.

Waite Jr., J.H., and 21 colleagues, 2005. Ion Neutral Mass Spectrometer (INMS) results from the first flyby of Titan. Science 308, 982–986.

Waite Jr., J.H., Young, D.T., Cravens, T.E., Coates, A.J., Crary, F.J., Magee, B., Westlake, J., 2007. The process of tholin formation in Titan's upper atmosphere. Science 316, 870–875.

Wilson, E.H., Atreya, S.K., 2004. Current state of modeling the photochemistry of Titan's mutually dependent atmosphere and ionosphere. J. Geophys. Res. 109, E06002. doi:10.1029/2003JE002181.

Yelle, R.V., Borggren, N., de la Haye, V., Kasprzak, W.T., Niemann, H.B., Müller-Wodarg, I., Waite Jr., J.H., 2006. The vertical structure of Titan's upper atmosphere from Cassini Ion Neutral Mass Spectrometer measurements. Icarus 182, 567–576.

Yelle, R.V., Cui, J., Mü ller-Wodarg, I.C.F., 2008. Eddy diffusion and methane escape from Titan's atmosphere. J. Geophys. Res. 113, E10003. doi:10.1029/2007JE003031.

Yung, Y.L., Allen, M., Pinto, J.P., 1984. Photochemistry of the atmosphere of Titan – Comparison between model and observations. Astrophys. J. 55, 465–506. doi:10.1086/190963.

Please cite this article in press as: Strobel, D.F. Molecular hydrogen in Titan's atmosphere: Implications of the measured tropospheric and thermospheric mole fractions. Icarus (2010), doi:10.1016/j.icarus.2010.03.003